

Rational Design of an Apoptosis-Inducing Photoreactive DNA Intercalator**

Nico Ueberschaar, Hans-Martin Dahse, Tom Bretschneider, and Christian Hertweck*

One of the greatest medicinal challenges is the treatment of cancer, which has recently become the leading cause of death in economically developed countries and the second leading cause of death in emerging nations.^[1] Natural products from plant, fungi, and bacteria represent the prime source of medicines that help to extend the life expectancy of patients.^[2] The most effective chemotherapeutics either interfere with the tumor cell cycle and division or bind to DNA and cause apoptosis through various downstream processes.^[3] This prominent mode of action is known for the bacterial metabolites chartreusin (**1**) and elsamicin A (**2**; Figure 1 a).^[4] Common to both of these polyketide glycosides is the pentacyclic aglycone named chartarin (Figure 1, highlighted in blue). This rare chromophore is capable of intercalating into DNA, thereby inhibiting RNA synthesis and causing radical-mediated single-strand scission of DNA.^[5] Moreover, **1** and **2** efficiently inhibit topoisomerase II, which is a prime target of chemotherapeutics that are used to treat human malignancies.^[5] Although **1** and synthetic prodrugs are highly effective against various cancer cell lines, such as murine leukemia, and melanoma cells,^[6] a challenge associated with such chemotherapeutics is that they typically lack selectivity against tumor cells and thus damage healthy tissue. A promising avenue that is currently being explored to decrease unwanted side effects is addressing tumors with light after systemic or local drug administration.^[7] Various leads have been developed for photodynamic therapy,^[8] yet the clinical use of these compounds is hampered by severe side effects. For example, hypericin and porphyrin-like photosensitizers generate reactive oxygen species, which cause unselective oxidative damage and light hypersensitivity.^[7,9] For the light-induced release of cytotoxic agents various UV-dependent systems have been explored, for example, doxorubicin prodrugs with photolysis activation.^[10] However, the mutagenic effect of short-wave irradiation is well-known, and it has

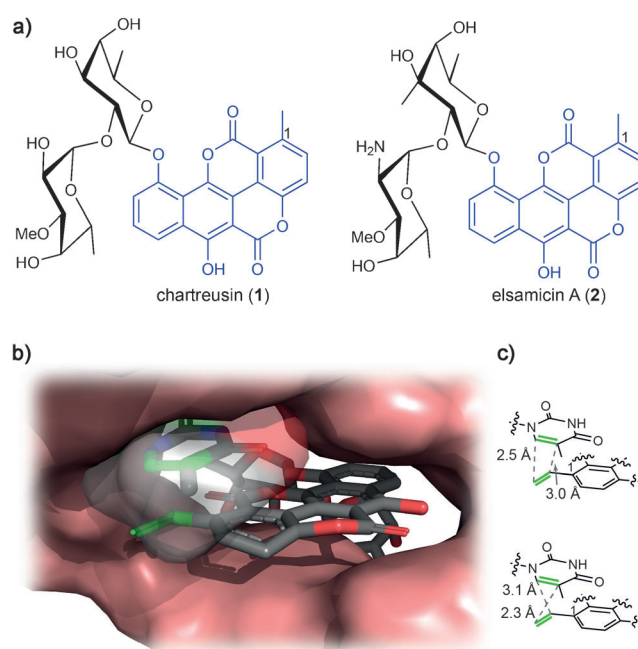


Figure 1. Structures of DNA intercalators and model of DNA binding. a) Structures of the antitumor agents chartreusin (**1**) and elsamicin (**2**) sharing the chartarin aglycone (highlighted in blue), b) Model of vinylchartreusin binding to DNA. View of the major groove shows proximity of the aglycone vinyl residue to thymine (double bonds marked in green). c) Distances of the thymine and vinyl carbon atoms measured in the model.

been shown that the UV light employed for photoactivation may induce secondary cancers.^[11] Examples of antitumoral agents that can be activated with visible light are scarce and encompass mainly photocleavable Pt or Ru complexes.^[12]

Herein we report the first successful tailoring of the potent chartarin pharmacophore by merging the strengths of molecular modeling, biosynthesis, and chemical synthesis. We demonstrate a viable chemobiosynthetic route to a novel vinyl-substituted chartreusin analogue, which forms covalent links to DNA upon mild photoactivation with visible light and which has a markedly higher antitumoral potency than the parent compound.

To rationally design chartreusin analogues with potentially improved potencies we modeled the structures of chartreusin and ring-substituted analogues into DNA and took into account current data on the multivalent, nonrandom binding properties. Since chartreusin preferentially binds to sequences containing CpG or TpG triplets,^[13] we docked it into a canonical B DNA between the T and G nucleotides of the sequence GCGTATGATGCG by using a standardized

[*] N. Ueberschaar, Dr. H.-M. Dahse, T. Bretschneider, Prof. Dr. C. Hertweck
Leibniz Institute for Natural Product Research and Infection Biology, HKI
Beutenbergstr. 11a, 07745 Jena (Germany)
E-mail: Christian.Hertweck@hki-jena.de
Prof. Dr. C. Hertweck
Friedrich Schiller University, Jena (Germany)

[**] We thank A. Perner for MS analysis, H. Heinecke for NMR measurements, T. Palenta for assistance in synthesis and E.-M. Neumann for assistance in biological assays. This work was supported by the Federal Ministry of Science and Technology (BMBF (Germany)).

Supporting information for this article is available on the WWW under <http://dx.doi.org/10.1002/anie.201302439>.

method.^[14] Interestingly, according to this model the glycoside residue fits into the minor groove of the DNA helix,^[13] thus supporting aglycone intercalation. We noted that the aryl methyl group would be placed next to the nucleobases. Likewise, a vinyl-substituted chartarin aglycone could be positioned in a way that the vinyl group and the double bond of the thymine were in proximity (Figure 1b,c). Consequently, such a nonnatural chartreusin derivative could in principle be capable of forming [2+2] photo adducts in analogy to the gilvocarcin V family of angucyclic polyketide glycosides, which are efficiently activated in the near UVA spectrum (398 nm).^[15] Since the absorption maxima of the chartarin chromophore are shifted to longer wavelengths compared to the angucyclins, we envisaged the possibility of generating an improved chartreusin analogue that can be activated with visible light. To test this hypothesis we aimed at preparing a chartreusin derivative substituted with a vinyl group.

Alteration of the alkyl substitution of chartreusin is challenging owing to the lack of protocols for the selective chemical derivatization of the methyl moiety. Since a total synthesis of chartreusin would be impracticable, we sought to harness the biosynthetic potential of the producing organism (Scheme 1). Specifically, we aimed at a mutasynthesis approach^[16] using a mutant that is unable to prepare the natural aglycone. On the basis of the known sequence of the

gene cluster coding for chartreusin (*cha*) biosynthesis from *Streptomyces chartreusis* and successful expression of the entire *cha* gene cluster in the heterologous host *Streptomyces albus*,^[17] genes coding for the type II polyketide synthase (PKS)^[18] were excised by PCR targeting.^[19] HPLC–MS monitoring showed that the *cha* PKS null mutant does not produce chartreusin or related metabolites (Figure 2, trace a).

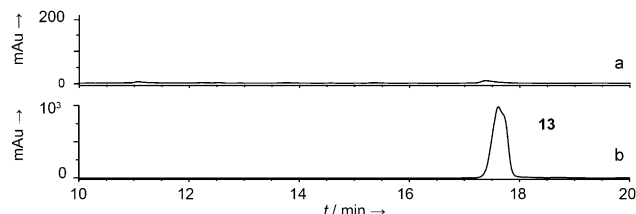
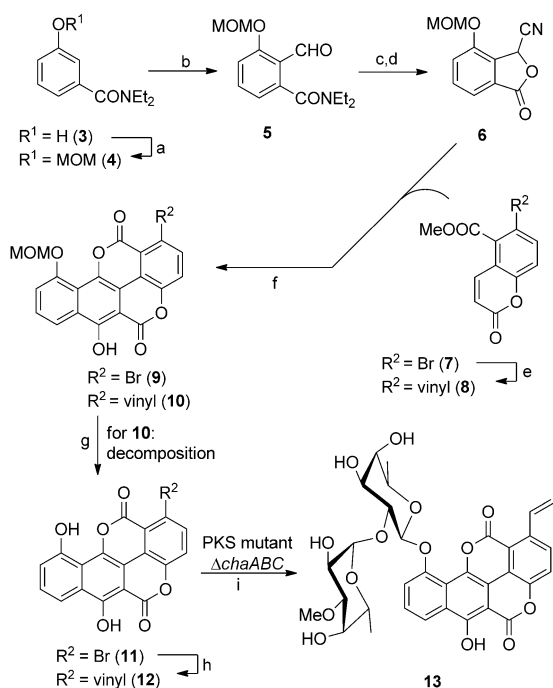


Figure 2. Mutasynthesis of the vinyl-substituted chartreusin analogue **13**. HPLC profiles ($\lambda = 400$ nm) of extracts from cultures of Δ PKS mutant supplemented with the following substrates: a) DMSO (negative control), b) synthetic vinylchartarin (**12**) in DMSO.

We next aimed at chemically complementing the mutant with the synthetic chartarin analogue. For the synthesis of the vinyl-substituted aglycone a Hauser tandem annulation strategy was employed, which has proven successful for the synthesis of the native aglycone^[20] (Figure 1, highlighted in blue). However, the corresponding vinyl-substituted aglycone could not be obtained by simply employing the vinyl-substituted coumarin **8**. Thus, we introduced a bromo substituent that could be replaced by another functional group at a later stage in the synthesis (Scheme 1). The bromo-substituted coumarin **7** proved to be a suitable reactant in the Hauser annulation, yielding bromochartarin (**9**) after deprotection. The coupling of **9** with a vinyl synthon, however, proved to be arduous, as reflected by the generally unsatisfactory examples of vinyl-group transfers onto (poly)-phenolic aryl bromides.^[21] We found that a Stille-type reaction with a bridged $[\text{Pd}(\text{dppp})\text{Cl}_2]$ catalyst in the presence of lithium chloride gave the best results (Scheme 1). Finally, the vinyl-substituted aglycone (**12**) was added to the Δ PKS mutant broth for biotransformation. Indeed, the formation of a new compound with the molecular mass of 652 amu pointed to the successful production of the vinyl derivative (Figure 2, trace b). The mutasynthesis was repeated at a preparative scale (18 mg starting material), providing a sufficient amount of vinylchartreusin (**13**; 100% turnover rate, 31% yield of isolated **13**) for a full characterization and biological evaluation. The identity of the new compound was verified by physicochemical data (HRESI-MS, ESI-MS², 1D-, 2D-NMR spectroscopy, UV/Vis spectroscopy).

Evaluation of the antiproliferative and cytotoxic activities of the new chartreusin variant **13** gave a surprising result. Compared to chartreusin, **13** exhibits only slightly lower activity against K-562 and HeLa tumor cells, and is about four times less active than chartreusin against the HUVEC cell line (Figure 3a). However, the situation changed dramatically under photoinducing conditions. For the photoactivation assay we employed a blue gallium(III) nitride (GaN) LED, taking advantage of its high spectral purity combined with



Scheme 1. Mutasynthesis of a chartreusin analogue. a–h) Synthesis of vinylchartarin (**12**). a) Methoxymethyl chloride (MOM-Cl), diisopropylethylamine, CH_2Cl_2 , 65%; b) $t\text{BuLi}$, N,N,N',N' -tetramethylethylenediamine, THF, DMF, 71%; c) trimethylsilyl cyanide, KCN, [18]crown-6, THF; d) AcOH , 60% (2 steps); e) vinylboronic acid pinacol ester, $[\text{Pd}(\text{PPh}_3)_4]$, dioxane/water, 92%; f) $t\text{BuOLi}$, THF, 71%; g) BBr_3 , CH_2Cl_2 , 100%; h) $[\text{Pd}(\text{dppp})\text{Cl}_2]$ ($\text{dppp} = 1,3\text{-bis}(\text{diphenylphosphanyl})\text{propane}$), LiCl , $n\text{Bu}_3\text{Sn-vinyl}$, DMF, 20%; i) biotransformation, 100% turnover rate, 31% yield of isolated **13**.

even illumination of the cell culture well plate. Furthermore, the emission wavelength (420 nm) perfectly matches with the absorption maximum of **13**, which is a prerequisite for efficient activations of the molecule (Figure 3b).

To validate the photoinduced activity of vinylchartreusin (**13**) in an antiproliferation assay we chose a colon adenocarcinoma cell line (HT-29). We compared standardized conditions in darkness with incubations in the presence of the blue LED cluster. Notably, the activity of **13** in conjunction with the LED proved to be 12-fold higher (GI_{50} 0.6 μM) than without light (GI_{50} 7.1 μM) (Figure 3d,e). In contrast, the activity of native chartreusin (**1**) was not affected by treatment with light. To investigate the fate of colon adenocarcinoma cells (HT-29) we visually monitored the microscopic appearance of the cancer cells after light exposure. Specifically, we exposed defined rows of the test plate after application of **13** for 2, 4, 6, 8, and 16 h with blue light and incubated them for a total duration of 72 h in darkness. Cell blebbing, a characteristic sign of apoptosis, was observed after irradiation for 2 h. After 4 h irradiation further signs of apoptosis, including chromatin condensation were detectable (Figure 3g). Longer irradiation did not have any further effect on the cells. To elucidate mechanistic details of DNA binding by **13**, an electrophoretic mobility assay (EMSA) was performed. For the irradiation of single samples in standard glassware we employed a laser, because it has a high spectral

purity similar to the LED combined with a reproducible high power density. Electrophoretic movement of the accurately defined DNA fragment was not altered in samples containing **1** or **13** without irradiation. In stark contrast, we observed a clear band shift to a higher molecular mass for DNA irradiated in the presence of **13** (Figure 4a, lane 7). Since this result strongly suggests that a covalent DNA adduct was formed, we explored the structural details of adduct formation. As a prerequisite, we optimized the irradiation procedure using a GaN laser diode as blue light source, which allowed us to photoactivate the chartreusin derivative under near physiological conditions. Buffered aqueous herring sperm DNA solution was treated with **13** and irradiated for 3 min with blue light. Through hydrolysis with hydrochloric acid the glycosides (DNA and chartreusin) were cleaved and the mixture was subjected to HPLC–HRMS analyses (Figure 4b). Our earlier modeling studies revealed that the vinyl residue is in proximity to the double bond of a thymine, and the plausible formation of two possible regioisomers (Figure 1c) was experimentally confirmed. According to UV absorption, HRMS data and HPLC retention times, two isomeric vinylchartarin thymine adducts (m/z 471.0838 [$M-H$] $^-$, 12.6 min, **T**^{#1}, and m/z 471.0835 [$M-H$] $^-$, 12.3 min, **T**^{#2}) were identified. Two additional vinylchartarin adducts were detected: adducts of vinylchartarin with guanine (9.2 min, m/z 456.0836 [$M-H$] $^-$, **G**[#]) and cytosine (9.7 min,

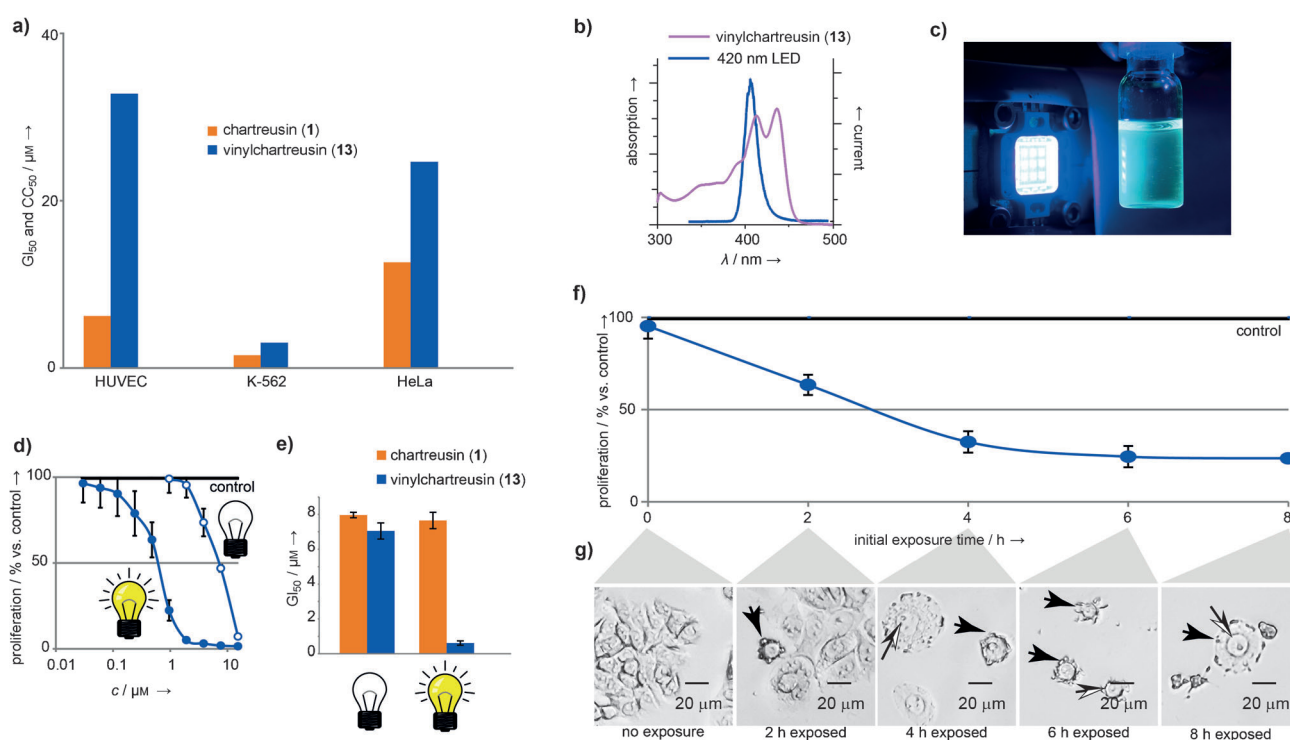


Figure 3. Evaluation of antiproliferative effects and induction of apoptosis. a) GI_{50} (HUVEC, K-562) and CC_{50} (HeLa) values for chartreusin and its vinyl-substituted analogue. GI_{50} = concentration required to cause 50% reduction in proliferation; CC_{50} = cytostatic concentration required to reduce cell growth by 50%. b) Overlay of absorption spectrum of **13** in presence of DNA and emission spectrum of the blue LED light source. c) Image of the LED light source and a vial containing chartreusin showing its fluorescence. d) Light-dependent antiproliferative effect on human colon adenocarcinoma cell line HT-29. Dose–response curve of **13** with and without light. e) Corresponding growth-inhibition values with and without light. f) Time-resolved effect of the inhibition of proliferation by vinylchartreusin (**13**) on HT-29 cells at a constant concentration ($c = 1.25 \mu\text{g mL}^{-1}$). g) Microscope images of the corresponding HT-29 cells show chromatin condensation (black/white arrowhead) and cell blebbing (black arrowhead) indicative of apoptosis.

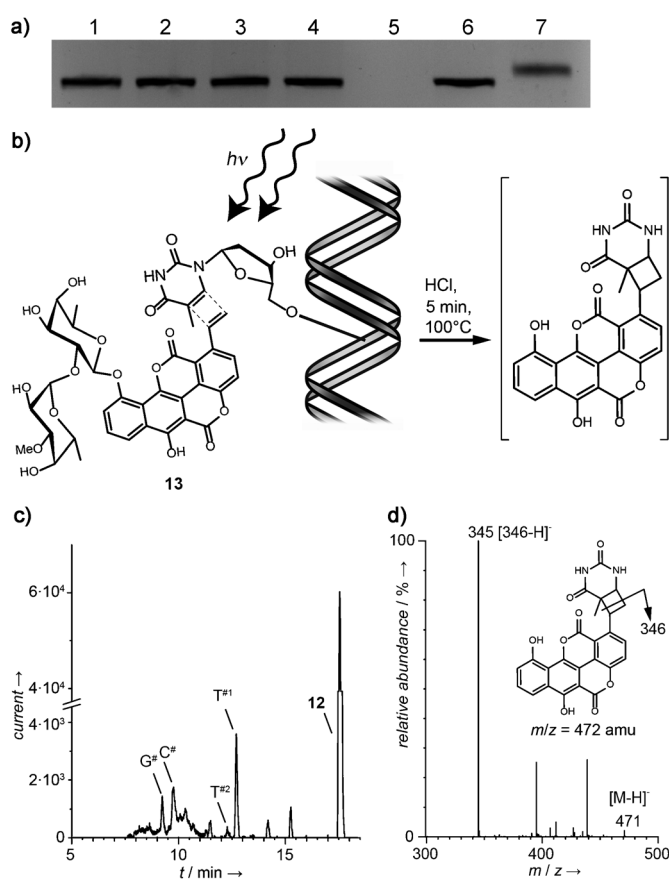


Figure 4. Light-induced DNA adduct formation. a) Agarose gel of 1.5 kb DNA fragment. Lanes 1, 2: DNA samples without supplement; lanes 3, 4: DNA incubated with chartreusin (**1**); lane 5: **13** without DNA; lanes 6, 7: DNA incubated with **13**; lanes 2, 4, 7: samples irradiated with blue light ($\lambda = 405$ nm). b) Illustration of [2+2] DNA photoadduct formation and acidic hydrolysis. c) HPLC–HRMS profile ($\lambda = 400$ – 420 nm) of herring sperm DNA treated with **13** and blue light ($\lambda = 405$ nm), followed by digestion with hydrochloric acid; **G#**: $m/z = 456$ amu, [2+2] adduct of **13** and guanine; **C#**: $m/z = 496$ amu, [2+2] adduct of **13** and cytosine; **T#1** and **T#2**: $m/z = 471$ amu, [2+2] adduct of **13** and thymine as well as recovered vinylchartarin aglycone **12**. d) MS² spectrum of thymine adduct **T#1**.

m/z 496.0903 [$M-H$][−], **C#**). The relative occurrence of the adducts (**T#1**/**T#2**/**G#**/**C#** = 1:0.08:0.36:0.62) indicates a strong preference to form thymine adducts, yet there is some flexibility in the photoreaction, likely owing to intercalation of the vinylchartreusin aglycone at different sites (Figure 4c,d).

In summary, we have explored a new chemobiosynthetic route towards a rationally designed, photoactivatable chartreusin analogue. To our knowledge, conversion of a fully synthetic polyphenolic core into the corresponding glycoside by mutasynthesis is unprecedented. This efficient route also granted the first (semi)synthetic access to a chartreusin analogue with a modified aglycone, and the novel apoptosis-inducing DNA intercalator can be activated by visible light, thus minimizing UV-induced mutations. Our study not only highlights the power of merging chemical and biochemical methods to generate complex, natural-product-derived anti-

tumor agents,^[22] but also reveals a lead that holds promise for curing skin cancers and tumors that are accessible with light probes.

Received: March 23, 2013

Published online: May 6, 2013

Keywords: antitumor agents · glycosylation · photoreaction · polyketides · *streptomyces chartreusis*

- [1] A. Jemal, F. Bray, M. M. Center, J. Ferlay, E. Ward, D. Forman, *CA-Cancer J. Clin.* **2011**, *61*, 69–90.
- [2] P. G. Grothaus, G. M. Cragg, D. J. Newman, *Curr. Org. Chem.* **2010**, *14*, 1781–1791.
- [3] A. C. Souza, A. de Fatima, R. B. da Silveira, G. Z. Justo, *Curr. Drug Targets* **2012**, *13*, 1072–1082.
- [4] a) J. Portugal, *Curr. Med. Chem.* **2003**, *3*, 411–420; b) M. Uramoto, T. Kusano, T. Nishio, K. Isono, K. Shishido, T. Ando, *Febs Lett.* **1983**, *153*, 325–328.
- [5] A. Lorico, B. H. Long, *Eur. J. Cancer* **1993**, *29A*, 1985–1991.
- [6] a) T. Tashiro, K. Kon, M. Yamamoto, N. Yamada, T. Tsuruo, S. Tsukagoshi, *Cancer Chemother. Pharmacol.* **1994**, *34*, 287–292; b) J. P. McGovern, G. L. Neil, S. L. Crampton, M. I. Robinson, J. D. Douros, *Cancer Res.* **1977**, *37*, 1666–1672.
- [7] W. M. Sharman, C. M. Allen, J. E. van Lier, *Drug Discovery Today* **1999**, *4*, 507–517.
- [8] J. P. Celli, B. Q. Spring, I. Rizvi, C. L. Evans, K. S. Samkoe, S. Verma, B. W. Pogue, T. Hasan, *Chem. Rev.* **2010**, *110*, 2795–2838.
- [9] F. E. Fox, Z. Niu, A. Tobia, A. H. Rook, *J. Invest. Dermatol.* **1998**, *111*, 327–332.
- [10] S. Ibsen, E. Zahavy, W. Wrasidlo, M. Berns, M. Chan, S. Esener, *Pharm. Res.* **2010**, *27*, 1848–1860.
- [11] a) J. Ramos, J. Villa, A. Ruiz, R. Armstrong, J. Matta, *Cancer Epidemiol. Biomarkers Prev.* **2004**, *13*, 2006–2011; b) S. Hu, F. C. Ma, F. Collado-Mesa, R. S. Kirsner, *Arch. Dermatol.* **2004**, *140*, 819–824.
- [12] a) B. S. Howerton, D. K. Heidary, E. C. Glazer, *J. Am. Chem. Soc.* **2012**, *134*, 8324–8327; b) S. J. Berners-Price, *Angew. Chem.* **2011**, *123*, 830–831; *Angew. Chem. Int. Ed.* **2011**, *50*, 804–805.
- [13] a) X. Salas, J. Portugal, *Febs Lett.* **1991**, *292*, 223–228; b) P. L. Hamilton, D. P. Arya, *Nat. Prod. Rep.* **2012**, *29*, 134–143.
- [14] C. G. Ricci, P. A. Netz, *J. Chem. Inf. Model.* **2009**, *49*, 1925–1935.
- [15] a) L. R. McGee, R. Misra, *J. Am. Chem. Soc.* **1990**, *112*, 2386–2389; b) Y. Q. Li, X. S. Huang, K. Ishida, A. Maier, G. Kelter, Y. Jiang, G. Peschel, K. D. Menzel, M. G. Li, M. L. Wen, L. H. Xu, S. Grabley, H. H. Fiebig, C. L. Jiang, C. Hertweck, I. Sattler, *Org. Biomol. Chem.* **2008**, *6*, 3601–3605; c) M. Greenstein, T. Monji, R. Yeung, W. M. Maiese, R. J. White, *Antimicrob. Agents Chemother.* **1986**, *29*, 861–866; d) R. K. Elespuru, S. K. Gonda, *Science* **1984**, *223*, 69–71.
- [16] a) J. Kennedy, *Nat. Prod. Rep.* **2008**, *25*, 25–34; b) S. Weist, R. D. Sussmuth, *Appl. Microbiol. Biotechnol.* **2005**, *68*, 141–150; c) A. Kirschning, F. Hahn, *Angew. Chem.* **2012**, *124*, 4086–4096; *Angew. Chem. Int. Ed.* **2012**, *51*, 4012–4022.
- [17] Z. Xu, K. Jakobi, K. Welzel, C. Hertweck, *Chem. Biol.* **2005**, *12*, 579–588.
- [18] C. Hertweck, A. Luzhetskyy, Y. Rebets, A. Bechthold, *Nat. Prod. Rep.* **2007**, *24*, 162–190.
- [19] Z. Xu, PhD thesis, Friedrich Schiller University Jena, **2008**.
- [20] D. Mal, A. Patra, H. Roy, *Tetrahedron Lett.* **2004**, *45*, 7895–7898.
- [21] a) M. S. Malamas, E. S. Manas, R. E. McDevitt, I. Gunawan, Z. B. Xu, M. D. Collini, C. P. Miller, T. Dinh, R. A. Henderson, J. C. Keith, H. A. Harris, *Curr. Med. Chem.* **2004**, *47*, 5021–5040;

- b) F. Shibahara, K. Nozaki, T. Matsuo, T. Hiyama, *Bioorg. Med. Chem. Lett.* **2002**, *12*, 1825–1827.
- [22] a) M. Ziehl, J. He, H.-M. Dahse, C. Hertweck, *Angew. Chem.* **2005**, *117*, 1226–1230; *Angew. Chem. Int. Ed.* **2005**, *44*, 1202–1205; b) M. Werneburg, B. Busch, J. He, M. E. A. Richter, L. K. Xiang, B. S. Moore, M. Roth, H. M. Dahse, C. Hertweck, *J. Am. Chem. Soc.* **2010**, *132*, 10407–10413; c) A. S. Eustáquio, B. S. Moore, *Angew. Chem.* **2008**, *120*, 4000–4002; *Angew. Chem. Int. Ed.* **2008**, *47*, 3936–3938; d) S. Eichner, T. Knobloch, H. G. Floss, J. Fohrer, K. Harmrolfs, J. Hermene, A. Schulz, F. Sasse, P. Spiteller, F. Taft, A. Kirschning, *Angew. Chem.* **2012**, *124*, 776–781; *Angew. Chem. Int. Ed.* **2012**, *51*, 752–757; e) T. Knobloch, K. Harmrolfs, F. Taft, B. Thomaszewski, F. Sasse, A. Kirschning, *ChemBioChem* **2011**, *12*, 540–547; f) F. Taft, K. Harmrolfs, I. Nickeleit, A. Heutling, M. Kiene, N. Malek, F. Sasse, A. Kirschning, *Chem. Eur. J.* **2012**, *18*, 880–886.
-